Journal of Applied Electrochemistry **34**: 879–884, 2004.

The effect of aluminum ions on the DC etching of aluminum foil

JONG-HO RYU[1], JONG HYUN SEO[2], JAE-HAN JEONG[3], SUNG-KAP KIM[1] and DONG NYUNG LEE[4]*
[1]*ILJIN Copper Foil Co., Ltd., Wolsan Industrial Complex, Nam-Myun Yongi-Gun, Chungcheongnam-Do, Korea*
[2]*Samsung Electronics Co., Ltd., San #24 Nongseo-Ri, Giheung-Eup Yongin-City, Gyunggi-Do, Korea*
[3]*Technology Development Team, Technology & Research Center, Korea Fire Equipment Inspection Corp. #136 Jigok-Ri, Giheung-Eup Yongin-City, Gyunggi-Do, Korea*
[4]*Research Institute of Advanced Materials and School of Materials Science and Engineering, Seoul National University, Seoul 151-742, Korea*
*(*author for correspondence, e-mail: dnlee@snu.ac.kr)*

Received 20 August 2003; accepted in revised form 23 March 2004

Key words: Al ion, chronopotentiometry, DC etching, electrochemical impedance, etch tunnel, linear sweep test

Abstract

A study has been made of the electrochemical etching of 99.99% aluminum foils at a current density of 50 mA cm^{-2} in $AlCl_3$–HCl solutions (1 M Cl^-) at 80 °C. The solutions were made by dissolving metallic aluminum into 1 M HCl solution, to give a Cl^- concentration of 1 M. The number density of etch tunnels and the homogeneity of tunnel length decreased, and the mean pit size and its standard deviation increased with increasing Al^{3+} concentration. The results were discussed based on potential transients at a current density of 50 mA cm^{-2}, current–potential curves at a scan rate of 10 mV s^{-1} and electrochemical impedance spectra.

1. Introduction

Electrochemical etching of aluminum foils is widely used in the manufacture of electrolytic capacitor electrodes, because it results in an increase in surface area, which in turn gives rise to an increase in the capacitance per foil volume [1–3].

The anodic dissolution of high-purity aluminum foil by direct current (DC) etching in aqueous chloride solutions above 60 °C produces high number densities (10^9–10^{12} m^{-2} of metal surface) of microscopic corrosion tunnels. These etch tunnels are 0.5–2 μm wide, square to round in cross-section and penetrate into the metal along the ⟨1 0 0⟩ directions with a constant width or taper as they penetrate [4]. The {1 0 0} pit surfaces and the ⟨1 0 0⟩ tunnel directions are related to the fact that the stability of the passive film depends on the orientation of substrate [4, 5]. During electrochemical DC etching, the etch pit width and tunnel length are influenced by the concentration of aqueous chloride [6], the electrolyte temperature [3, 6–11], the current density [2, 12–15], and additives [16–21].

During etching, aluminum dissolves in Cl^--containing solutions to form Al^{3+} with the Cl^- concentration remaining constant. Therefore, it is important to study the effect of Al^{3+} concentration in constant Cl^- concentration solutions on etching behavior. Recently, it has been reported that the addition of $AlCl_3 \cdot 6\ H_2O$ in aqueous Cl^- solution decreases the pit size and the etch tunnel length, but increases the pit density [22, 23]. In these cases, the effects of Al^{3+} and Cl^- were simultaneously involved. In order to better understand the role of Al^{3+} in the etching of pure aluminum in Cl^- containing solutions, it is appropriate to study the effect of Al^{3+} at constant Cl^- concentration.

The purpose of this work is to investigate the effect of Al^{3+} concentration in $AlCl_3$–HCl solutions with the Cl^- concentration remaining constant on the initiation and growth stages of aluminum, etching and to discuss the results based on the morphology of etched layers, chronopotentiometric and potential linear sweep data and AC impedance curves.

2. Experimental

Specimens for etching were prepared from a 99.99% Al capacitor-grade foil of 110 μm thickness. The foil had a strong cubic-texture, {0 0 1}⟨1 0 0⟩, so that etch tunnels grew normal to the surface.

The specimens were immersed in 2 M H_3PO_4 at 50 °C for 30 s, rinsed under deionized water and then blown dry with hot air. The dried specimen was mounted in a holder having an opening of 1 cm^2, for current flow. Electrode potentials were recorded relative to a saturated calomel electrode (SCE).

Table 1. Composition of etching solutions (1 M Cl^-)

Al^{3+}, g l^{-1}	0	1	3	5	7	9
HCl, M	1	0.889	0.666	0.444	0.222	0
$AlCl_3$, M	0	0.037	0.111	0.185	0.259	0.334

The etching solutions were made by dissolving pure aluminum foil in 5 M HCl solution at about 70 °C, followed by dilution with deionized water. The Al^{3+} concentration in the solution varied between 0 and 9 g l^{-1} (Table 1). An Al^{3+} concentration of 9 g l^{-1} is the maximum value that can be made in 1 M HCl solution. $AlCl_3$–HCl solutions with Cl^- concentration of 1 M will be referred to as Al^{3+}–H^+–1 M Cl^- solutions.

The chronopotentiometric and linear sweep experiments were conducted on the native oxide film-covered Al foil specimens in Al^{3+}–H^+–1 M Cl^- solutions at 80 °C, 50 mA cm^{-2} with a potentiostat/galvanostat. AC impedance measurements were carried out on the native oxide film-covered Al foil specimen in 0–7 g l^{-1} Al^{3+}-containing 1 M Cl^- solutions at 80 °C. A single sinusoidal potential of 5 mV peak to peak was superimposed on the rest potential over frequencies of 1–10^5 Hz. When the steady state current was attained, the electrochemical impedance was measured with an impedance analyzer (Zahner IM6D).

3. Results

3.1. *Morphologies*

The mean size and distribution were measured over 100 pits on a SEM image magnification of 4000×. Figure 1 shows the pit size distributions on aluminum foil etched in 0–7 g l^{-1} Al^{3+}-containing 1 M Cl^- solutions at 80 °C and at a current density of 50 mA cm^{-2} for 10 min, from which the mean pit size and its standard deviation were calculated as a function of Al^{3+} concentration. The results are shown in Figure 2. It can be seen that the mean pit size and its standard deviation increase with increasing Al^{3+} concentration. The increase in standard deviation of pit size may be interpreted as the decrease in pit-size homogeneity.

An increase in Al^{3+} concentration means a decrease in H^+ concentration at the same time (Table 1). Therefore, the H^+ concentration will not be mentioned, unless otherwise necessary.

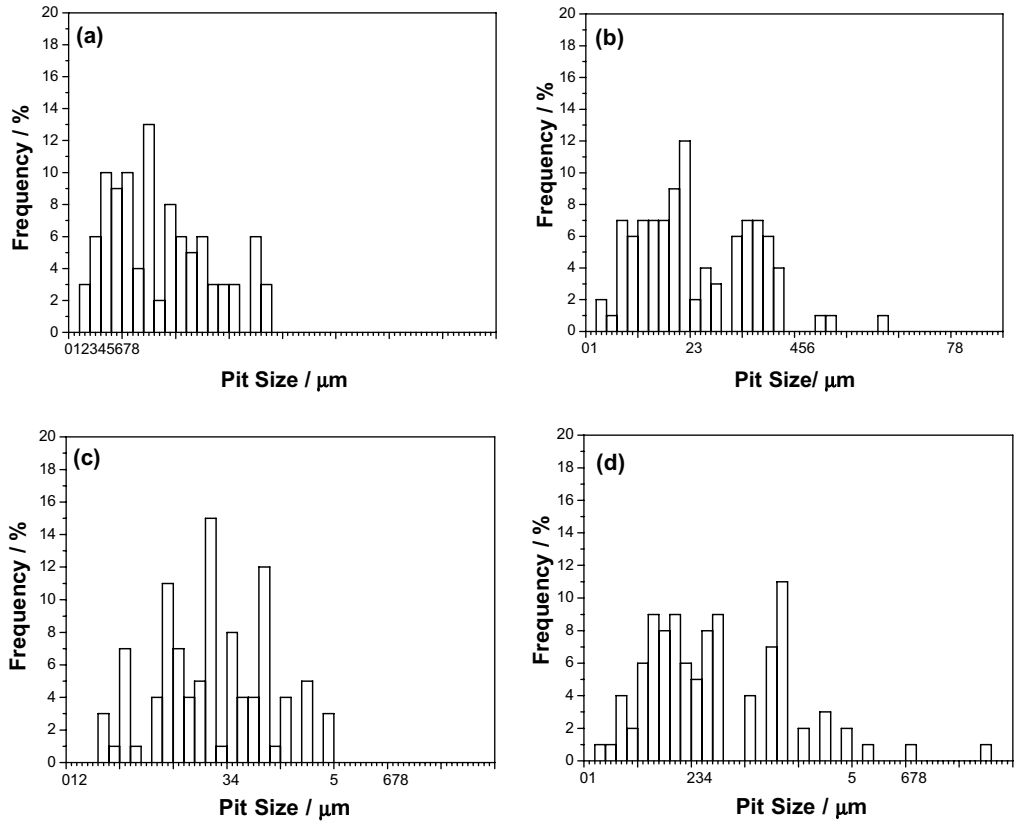

Fig. 1. Size distributions of 100 pits on aluminum foil etched at 50 mA cm^{-2} for 10 min in (a) 0, (b) 3, (c) 5 and (d) 7 g l^{-1} Al^{3+} -containing 1 M Cl^- solutions at 80 °C.

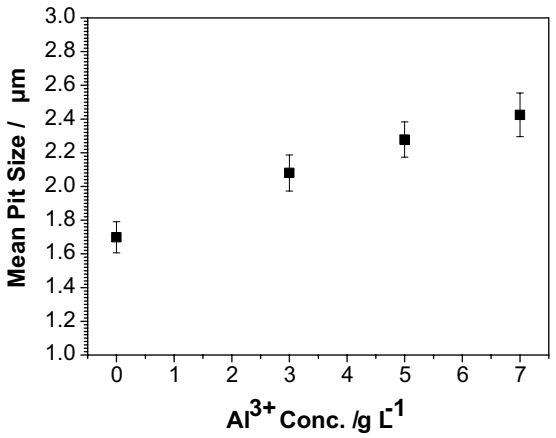

Fig. 2. Mean size of pits on aluminum foil etched in 80 °C 1 M Cl^- solution at 50 mA cm^{-2} for 10 min as a function of Al^{3+} concentration.

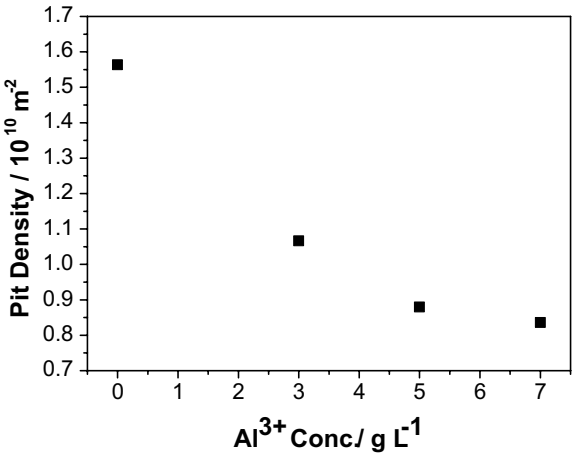

Fig. 3. Pit density of aluminum foil etched in 80 °C 1 M Cl^- solution at 50 mA cm^{-2} for 10 min as a function of Al^{3+} concentration.

Figure 3 shows the variation of pit number densities after etching in 0–7 g l^{-1} Al^{3+}-containing 1 M Cl^- solutions at 80 °C, 50 mA cm^{-2} for 10 min. The pit number densities were measured from SEM micrographs of 50 000 μm^2 taken after electropolishing in a solution consisting of 10% perchloric acid and 90% ethanol at −15 °C, 16 V for 15 s. The pit number density decreases with increasing Al^{3+} concentration.

SEM micrographs of the cross-sections of foils etched in Al^{3+}–H^+–1 M Cl^- solutions at 80 °C are shown in Figure 4. As the concentration of Al^{3+} increases, the tunnel pit density decreases and the axial growth of tunnel pit is suppressed.

The results of Figures 1–4 indicate that an increase in Al^{3+} concentration in the solution decreases the number of pit nucleation sites and in turn increases the current density per pit, resulting in an increase in pit size. In other words, the pitting corrosion of aluminum foil decreases with increasing Al^{3+} concentration in 1 M Cl^- solution.

3.2. *Chronopotentiometry*

Figure 5 shows a schematic diagram of the electrode potential transient in the initial DC etching. When a constant current is applied, the potential increases up to the maximum value (E_b), after a time τ_b, due to double layer charging [24] and/or a continuous aluminum chloride film forming at high anodic potentials [25, 26]. After the maximum, there is a very sharp decay down to the potential plateau E_s. Figure 6 shows the electrode potential and SEM morphology of the aluminum specimen as a function of etching time in 9 g l^{-1} Al^{3+}-containing 1 M Cl^- solution at 50 mA cm^{-2}. Pitting corrosion does not take place until the maximum potential E_b. Therefore, E_b is the breakdown potential, τ_b is the breakdown time, E_s is the steady-state potential and τ_s is the time of steady-state onset.

Figure 7 shows potential transients for the aluminum specimen obtained upon application of a constant current density of 50 mA cm^{-2} in 0–9 g l^{-1} Al^{3+}-containing 1 M Cl^- solutions at 80 °C. As the Al^{3+} ion

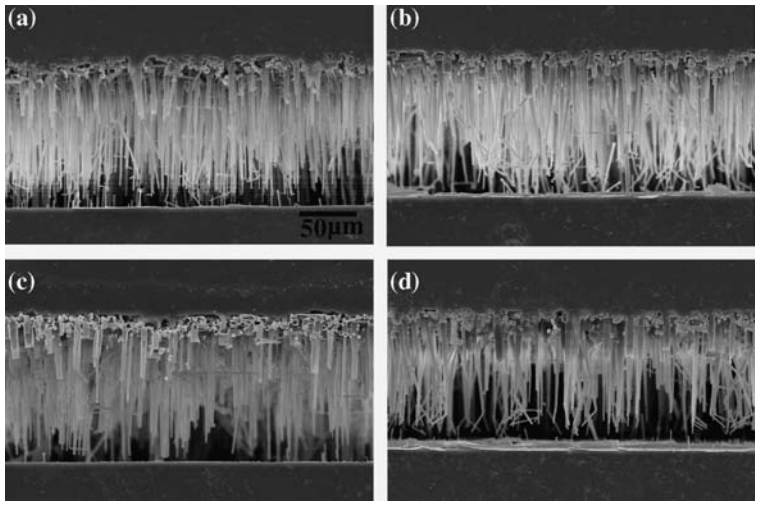

Fig. 4. Cross-sectional morphologies of aluminum foils etched at 50 mA cm^{-2} for 10 min in (a) 0, (b) 3, (c) 5 and (d) 7 g l^{-1} Al^{3+}-containing 1 M Cl^- solutions at 80 °C.

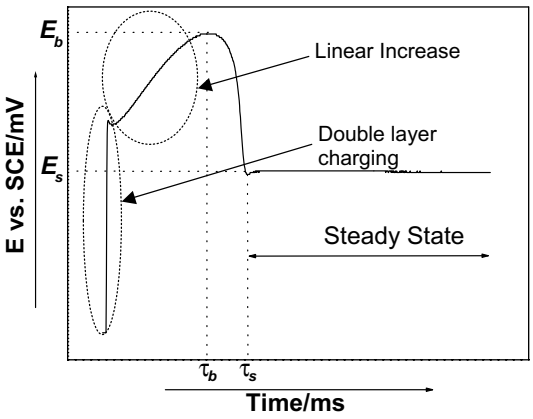

Fig. 5. Schematic diagram of potential transient obtained by chronopotentiometric measurement.

concentration increases, E_b, τ_b, E_s and τ_s increase. The breakdown potential shifts in the noble direction with increasing Al^{3+} concentration. This indicates that the aluminum–chloride film thickness increases with increasing Al^{3+} ion concentration and/or that the Cl^- ion activity, which is responsible for the pitting corrosion of aluminum, decreases. The steady-state potential shifts in the noble direction with increasing Al^{3+} ion concentration. This potential shift is caused by the occurrence of some hindrance to the anodic processes on aluminum. A major factor is thought to be repassivation.

3.3. *Cyclic Voltammetry*

Figure 8 shows the effect of Al^{3+} concentration on the cyclic voltammetric curve of non-etched aluminum foil in 1 M Cl^- solution at a potential sweep rate of 10 mV s^{-1} with potentials between −1.0 and −0.7 V vs SCE. Relevant parameters that can be determined from the linear sweep current–potential curves include the pitting potential (E_p), the repassivation potential (E_{pp}) and the magnitude of the anodic current. On sweep reversal, the backward curves lay at higher currents than the forward curves. The anodic current density decreases with increasing Al^{3+} concentration. The pitting and repassivation potentials increase with increasing Al^{3+} ion concentration. The initiation of pits and the hindrance of anodic processes on aluminum are not controlled only by Cl^-. In order to see the effect of chemical dissolution in 1 M Cl^- solutions including different Al^{3+} concentrations, $0.1 \times 0.3 \times 80$ mm size aluminum specimen was dissolved in each of the solutions at 95 °C. The dissolution times of the aluminum specimen in 500 ml solutions including 0, 3, and 7 g l^{-1} Al^{3+} were 14 h 25 min, 20 h 45 min, and 22 h 50 min, respectively. This result indicates that the Cl^- activity decreases with increasing Al^{3+} concentration.

3.4. *AC impedance spectra*

Figure 9 shows the impedance behavior of a non-etched aluminum foil in 0–7 g l^{-1} Al^{3+}-containing 1 M Cl^- solutions at 80 °C, rest potentials with an AC voltage-range of 5 mV. The capacitance of aluminum film in an electrolyte can be influenced by a passive film and an electric double layer. The film and the layer can be modeled to be serially connected. The total capacitance C_{total} of the circuit can be expressed as

$$\frac{1}{C_{total}} = \frac{1}{C_{film}} + \frac{1}{C_{dl}} \quad (1)$$

where C_{film} and C_{dl} are the capacitance of the film and the capacitance of the double layer. C_{dl} is in the order of

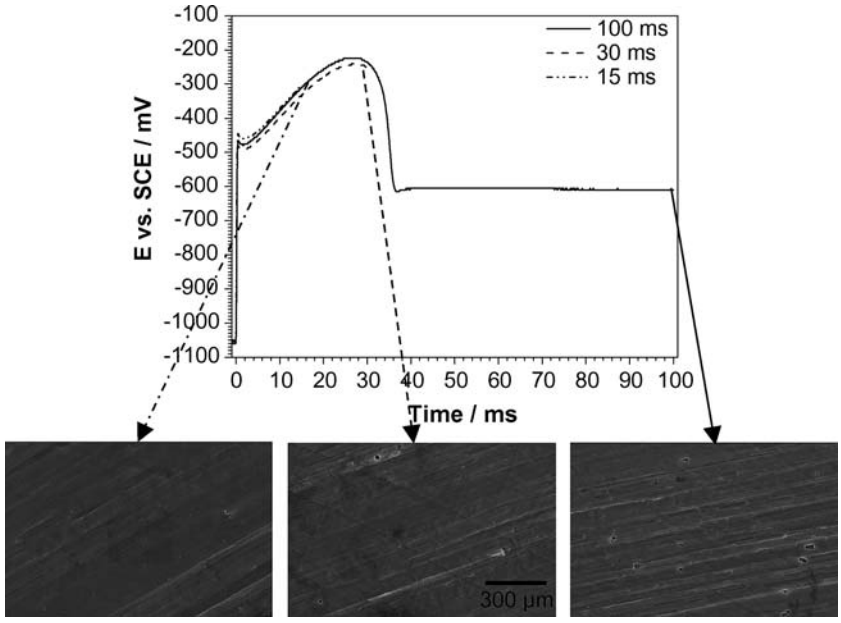

Fig. 6. SEM micrographs and potential transients for aluminum foil in 9 g l^{-1} Al^{3+}-containing 1 M Cl^- solution at 80 °C at 50 mA cm^{-2}.

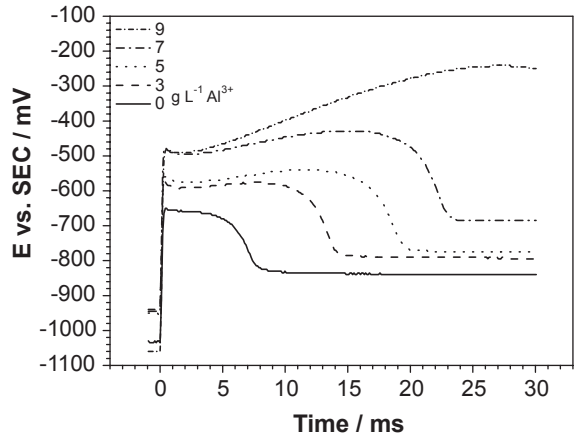

Fig. 7. Potential transients for aluminum foil in 0–9 g l^{-1} Al^{3+}-containing 1 M Cl^- solutions at 80 °C, 50 mA cm^{-2}.

40–60 μF cm^{-2}, which is generally much larger than C_{film}, C_{total} being approximated by C_{film} [27, 28]. Therefore, the circuit for the impedance spectra may be approximated by the equivalent circuit shown in Figure 9(a).

The solution resistance increases and the capacitance decreases with increasing Al^{3+} concentration. The decrease in film capacitance indicates an increase in the aluminum chloride film thickness.

4. Discussion

Nguyen and Foley [29] and Foley and Nguyen [30] suggested that the chemical composition of pure aluminum oxide film changed due to Cl^- incorporation into the film in the pre-pitting stage below the pitting potential (E_{pit}). The incorporated Cl^- ions form transitory compounds such as $Al(OH)_2Cl$, $Al(OH)Cl_2$ and $AlCl_3$ that are known to be consecutively formed in Cl^--containing solution. The transitory compounds are dissolved as an Al complex ion of $AlCl_4^-$ at a potential higher than the pitting potential, thereby resulting in pit initiation. Therefore, the existence of Al^{3+} in the solution prior to etching decreases the possibility of Cl^- adsorption on the aluminum surface during etching.

According to Herbert and Alkire [8], etch tunnels do not grow if $AlCl_3$ solution etchant is saturated with $AlCl_3$. It is expected that the resistance to transport of $AlCl_3$ increases with increasing tunnel length, and tunnels stop growing when their tips become saturated with $AlCl_3$.

The slope of the polarization curves at potentials above E_p in Figure 8 is related to the solution conductivity between the reference electrode and the working electrode. The resistances calculated from the slopes of the polarization curves are almost the same as the data measured from the impedance spectra in Figure 9(a) as shown in Figure 9(b). The solution resistance increases with increasing Al^{3+} concentration. The most dominant charge carrier in the bath is thought to be hydrogen ions. The decrease in solution conductivity is caused by a decrease in hydrogen ion concentration in the bath.

5. Conclusions

This study of the electrochemical etching of 99.99% aluminum foils in 0 to 9 g l^{-1}-containing 1 M Cl^- solution at 80 °C leads to the following conclusions.

(1) As the Al^{3+} concentration increased, the mean pit size increased, and the pit density decreased.
(2) The pitting, repassivation, breakdown and dissolution potentials increased with increasing Al^{3+} concentration.

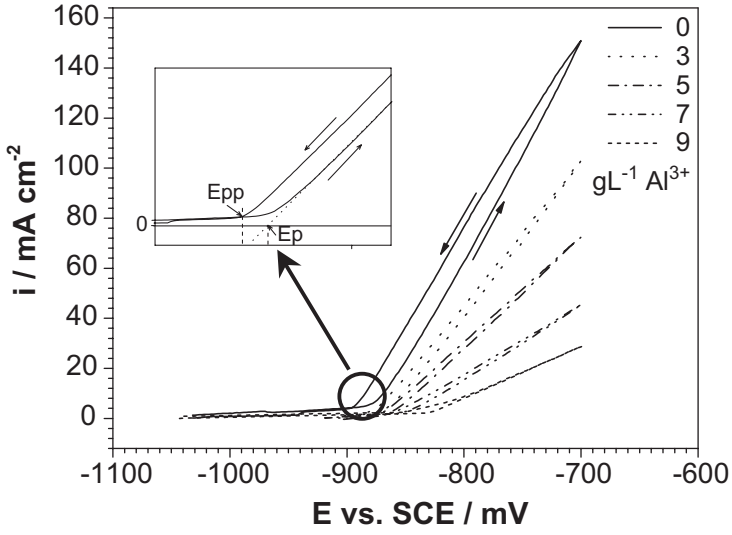

Fig. 8. Current *i*–potential *E* curves for aluminum foil in 0–9 g l^{-1} Al^{3+}-containing 1 M Cl^- solutions at 80 °C, scan rate of 10 mV s^{-1}. Forward and backward scan directions are indicated by arrows. E_p and E_{pp} indicate pitting and repassivation potentials, respectively.

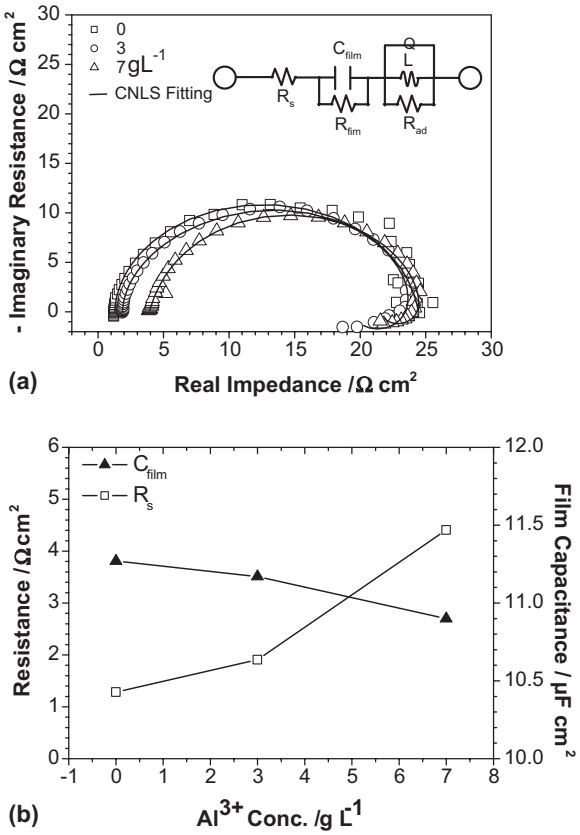

Fig. 9. Effect of Al^{3+} concentration on electrochemical impedance spectra of non-etched aluminum foil measured at open circuit in 1 M Cl^- solutions at 80 °C. (a) Nyquist plots and equivalent circuit are used to calculate, (b) film capacitance C_{film} by complex nonlinear least square (CNLS) fitting and solution resistance R_s (real impedance at zero imaginary impedance).

(3) The solution resistance increased, and the capacitance decreased with increasing Al^{3+} concentration.
(4) Al^{3+} ions suppress the initiation of pit on a passive film-covered aluminum foil and the growth of pre-existing pits.

Acknowledgement

This study was supported by Texture Control Laboratory (NRL), Seoul National University. The authors are grateful for many helpful comments from the referees of this manuscript.

References

1. M.S. Hunter, *J. Electrochem. Soc.* **117** (1970) 1215.
2. C.G. Dunn, R.B. Bolon, A.S. Alwan and A.W. Stirling, *J. Electrochem. Soc.* **118** (1971) 381.
3. N.F. Jackson, *Electrocomp. Sci. Technol.* **2** (1975) 33.
4. J.H. Jeong, C.-H. Choi and D.N. Lee, *J. Mater. Sci.* **31** (1996) 5811.
5. J.H. Seo, J.-H. Ryu and D.N. Lee, *J. Electrochem. Soc.* **150** (2003) B433.
6. D. Goad, *J. Electrochem. Soc.* **144** (1997) 1965.
7. R.S. Alwitt, H. Uchi, T.R. Beck and R.C. Alkire, *J. Electrochem. Soc.* **131** (1984) 13.
8. K. Hebert and R. Alkire, *J. Electrochem. Soc.* **135** (1988) 2447.
9. U.S. Patent, 4474657.
10. U.S. Patent, 4518471.
11. U.S. Patent, 4525249.
12. J.-H. Jeong, PhD thesis, Seoul National University, Korea (1993).
13. M.S. Hunter, *Electrochem. Technol.* **1** (1963) 151.
14. R. Bakish, E.Z. Borders and R. Kornhaas, *J. Electrochem. Soc.* **109** (1962) 791.
15. R. Bakish and R.J. Kornhaas, *Electrochem. Technol.* **6** (1968) 192.
16. J. Flis and L. Kowalczyk, *J. Appl. Electrochem.* **25** (1995) 501.
17. A. Hibino, M. Tamaki, Y. Watanabe and T. Oki, *J. Japan Inst. Light Metals* **42** (1992) 440.
18. A. Hibino, M. Tamaki, Y. Watanabe and T. Oki, *Sumitimo Light Metal Technical Rep.* **33** (1992) 236.
19. W.J. Rudd, PhD thesis, University of Leeds (1978).
20. W.-J. Lee and S.-I. Pyun, *Electrochim. Acta* **45** (2000) 1901.
21. I.L. Rozenfeld and I.S. Danilov, *Corr. Sci.* **7** (1967) 129.
22. N. Koura, F. Matsumoto, H. Saruwatari, S. Kitahara, Y. Idemoto, T. Yamasaki, M. Furukawa and H. Uchi, *J. Surf. Finishing. Soc. Japan* **53** (2002) 154.
23. N. Koura, F. Matsumoto, T. Yamasaki, H. Saruwatari, Y. Idemoto, S. Kitahara, S. Ono and H. Uchi, *J. Surf. Finishing. Soc. Japan* **54** (2003) 217.
24. R.M. Stevanovic, A.R. Despic and D.M. Dražić, *Electrochim. Acta* **33** (1988) 397–404.
25. T.R. Beck, *Electrochim. Acta* **29** (1984) 485.
26. W.M. Moore, C. Chen and G.A. Shrin, *Corrosion* **40** (1984) 644.
27. S.R. Morrison, 'Electrochemistry at Semiconductor and Oxidized Metal Electrode', (Plenum Press, New York, 1980), p. 119.
28. J.R. Scully, *in* J.R. Scully, D.C. Silverman and M.W. Kendig (Eds.), *Elecrochemical Impedance*: *Analysis and Interpretation, ASTM STP 1188*, (ASTM, Philadelphia, 1993), pp. 276–296.
29. T.H. Nguyen and R.T. Foley, *J. Electrochem. Soc.* **126** (1979) 1855.
30. R.T. Foley and T.H. Nguyen, *J. Electrochem.* Soc. **129** (1982) 464.